Sensors and Actuators B 220 (2015) 107–114

Contents lists available at ScienceDirect

Sensors and Actuators B: Chemical

journal homepage: www.elsevier.com/locate/snb

Highly sensitive biochemical sensor comprising rectangular nanometal arrays

Yue-Jing He*

Department of Electronic Engineering, National Chin-Yi University of Technology, Taichung 41170, Taiwan, ROC

ARTICLE INFO

Article history:
Received 24 March 2015
Received in revised form 20 May 2015
Accepted 21 May 2015
Available online 3 June 2015

Keywords:
Finite element method
Eigenmode expansion method
Perfectly matched layer
Perfectly reflecting boundary condition
Object meshing method
Boundary meshing method

ABSTRACT

This paper proposes a novel design for a highly sensitive high-resolution localized surface plasmon resonance (LSPR) biochemical sensor. The geometrical structure of the sensor consists of three segments. The first segment comprises single-mode fibers located in the output and input ends of the sensor. The second and third segments comprise rectangular nanometal arrays and serve as the analyte regions of the sensor; the amount of displacement between these two segments is one rectangular nonmetal particle. We integrated two breakthrough methods, the object meshing method and the boundary meshing method, with the finite element method to effectively improve the accuracy of simulation outcomes and reduce the amount of time and memory required for performing calculations. Subsequently, we constructed the proposed LSPR biochemical sensor, and the results indicated that the proposed sensor exhibited excellent geometric structure and spectral characteristics. Specifically, the sensor is short (approximately 240 μm) and features high resolution (approximately −130 dB) and high sensitivity (approximately 126,849.1333 nm/RIU).

1. Introduction

In recent years, topics related to surface plasmon resonance (SPR) sensors have attracted substantial attention from scientists, and SPR sensors have been applied in various fields. Generally, SPR sensors can be classified into two categories. The first category comprises propagating surface plasmon resonance (PSPR) sensors with propagation capability. In such sensors, an SPR wave is excited, travels along the metal–analyte interface, and results in both energy propagation and energy loss. An SPR wave forms when the electrons in the metal absorb the energy of an incident light at a specific wavelength; subsequently, the resonant oscillation of the electrons occurs at the metal–analyte interface. The formation of such a wave at the metal–analyte interface enables PSPR sensors to be highly sensitive to changes in the refractive index of an analyte. Therefore, PSPR sensors have been extensively applied in several fields including biology, genetic engineering, and biochemistry [1–15]. The second category comprises localized surface plasmon resonance (LSPR) sensors that have no propagation capability. Such sensors are composed of nanometer-sized metal particles that are insufficiently large for excited LSPR wave propagation. When electrons in the nanometer-sized metal particles of an LSPR sensor absorb the energy of an incident light at a specific wavelength, the resonant oscillation of the electrons occurs at the metal particle–analyte interface and in the space between the metal particles.

Consequently, an LSPR sensor with no propagation capability features more resonance regions than does a PSPR sensor with propagation capability; this characteristic considerably increases the sensitivity of LSPR sensors to changes in target analytes [16–21]. Thus, LSPR sensors have been adopted in numerous fields including chemistry, biochemical sensing, label-free detection, and optoelectronics [22–31].

In our previous studies, we have applied the finite element method (FEM) and eigenmode expansion method (EEM) to design high-efficiency PSPR and LSPR biochemical sensors featuring various architectures [1,16–18]. To improve the accuracy of numerical calculation and reduce the error between simulations and practical operations, we modified the FEM by integrating it with a perfectly matched layer (PML) and perfectly refraction boundary (PRB). However, the FEM developed in our previous studies exhibited major disadvantages. Specifically, in the current numerical simulation methods, uniform triangular meshing is typically the primary technique used. The process of designing PSPR and LSPR biochemical sensors involves installing nanometer-sized metal objects and micrometer-sized waveguide objects in sensor segments. When the uniform triangular meshing method is applied to mesh sensor segments, to ensure that the nanometer-sized

* Tel.: +886 4 23924505; fax: +886 4 23926610.
E-mail address: yuejing@ncut.edu.tw

http://dx.doi.org/10.1016/j.snb.2015.05.068
0925-4005/

metal objects exhibit desirable meshing resolutions, considerable memory space and calculation time are wasted. Therefore, in this paper, we propose two innovative meshing techniques, namely, the object meshing method (OMM) and boundary meshing method (BMM). In the OMM, various resolutions can be used to mesh objects of dissimilar sizes, thereby reducing the amount of unnecessary meshes. In the BMM, high meshing resolutions are applied to the boundary between objects to accurately identify boundary locations and object parameters. The purpose of the present study was to design and analyze a highly sensitive LSPR biochemical sensor by using FEM integrated with OMM and BMM. The results of numerical simulations indicated that the proposed sensor performed excellently and featured the advantages of a short length (approximately 240 μm), high resolution (approximately −130 dB), and high sensitivity (approximately 126,849.1333 nm/RIU).

The remainder of this paper is organized as follows. Section 2 comprehensively introduces the proposed LSPR biochemical sensor, describing the geometrical objects, structural parameters, and material characteristics. In addition, two-dimensional (2D) and three-dimensional (3D) illustrations of the sensor are presented to clarify the arrangements of the rectangular nanometal arrays and the operational principles of the sensor. Finally, the practical aspects of the sensor are discussed and explained.

Section 3 details the techniques (i.e., the PML, PRB, OMM, and BMM) that were integrated with the FEM. According to mathematics, the obtained modes must be pairwise orthogonal. However, according to a numerical simulation method, the orthogonality of modes obtained using the FEM is never 0 because of the limited server memory space and calculation time. In other words, calculation errors are unavoidable when the numerical simulation method is used to perform simulation calculations. Thus, in this study, we used our previously proposed error evaluation standard for determining acceptable calculation errors. Specifically, the meshing resolution applied to the FEM must result in an orthogonality value of less than −40 dB for an obtained mode [16,17]. This section also presents 2D power distribution graphs of the core modes (HE_{11}), discrete LSPR waves, and discrete radiation modes solved using the FEM. According to these graphs, the SPR phenomenon occurred on the surface of and in the space between the metal nanoparticles. This characteristic primarily enables the high sensitivity of the proposed sensor.

Section 4 introduces the EEM, which is based on the Fourier series expansion theory. In the simulation calculation process, the EEM enables the optical wave to propagate energy in the biomedical sensor. According to the Fourier series expansion principle, calculation errors are unavoidable when the amount of expansion bases is insufficient. Therefore, according to our error evaluation standard, the number of modes used in the EEM must be sufficient to ensure that the overall energy loss of the sensor is less than −40 dB [16,17].

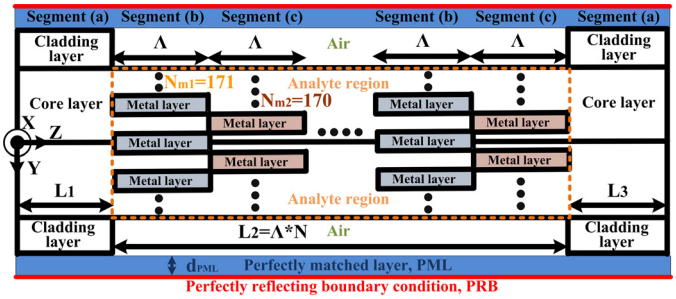

Fig. 2. 2D (*Y*–*Z*) structural illustration of LSPR biochemical fiber sensor.

Section 5 describes designing and analyzing the proposed sensor according to six design and analytical procedures. The results of the simulation are presented as graphs, including the graphs of excited surface plasmon waves, sensitivity analysis, and resolution spectrum analysis. In addition, to investigate the excellent performance of the proposed sensor, its architecture was compared with that of the novel D-shape LSPR fiber sensor [18] and high-performance LSPR biochemical fiber sensor [16].

Section 6 summarizes the proposed sensor and the innovative OMM and BMM. The results confirmed that the proposed sensor performed excellently and had the advantages of a short length (approximately 240 μm), high resolution (approximately −130 dB), and high sensitivity (approximately 126,849.1333 nm/RIU).

2. Novel LSPR biochemical sensor

The novel and highly sensitive LSPR sensor proposed in this study comprises three structurally dissimilar segments. Figs. 1–3 illustrate the 3D, 2D (*Y*–*Z*), and 2D (*X*–*Y*) geometrical structures of these segments, respectively. Segment (a) comprises single-mode fibers and is located on the input and output ends of the biochemical sensor. The procedures involved in constructing Segment (b) are outlined as follows. First, an etching process was applied to the cladding layer of the sensor by engraving a D-shaped cavity without affecting the core layer of the sensor. Next, rectangular nanogold particles were arranged in arrays and plated on the flat surface of the D-shaped cavity. The line extending from the center of the cross-sectional area of the core layer was used as the datum line for arranging the nanometal particles; the nanogold particles were symmetrically arranged on both sides of the datum line, and the duty cycle was 0.5. The procedures used for constructing Segment (c) were similar to those used for Segment (b); the two segments differed only in the arrangements of the nanogold arrays. Specifically, in each column of Segment (b), nanogold particles summing to an odd number were symmetrically arranged on both side of the datum line. In each column of Segment (c), nanogold particles

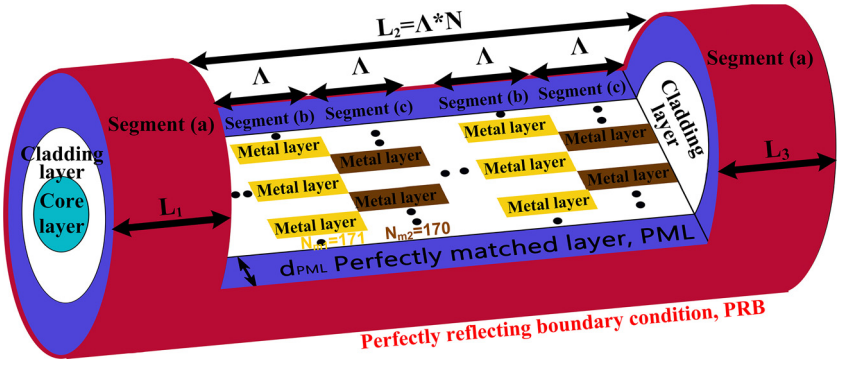

Fig. 1. 3D structural illustration of LSPR biochemical fiber sensor.